



	<b>Experiment title:</b> Nano-diffraction at individual SiGe/Si island clusters and InGaAs/GaAs quantum dot molecules	<b>Experiment number:</b> SI-2364
<b>Beamline:</b> ID10B	<b>Date of experiment:</b> from: 22.06.2011 to: 25.06.2011	<b>Date of report:</b> 05.03.2013
<b>Shifts:</b> 9	<b>Local contact(s):</b> Dr. Manfred Burghammer	<i>Received at ESRF:</i>
<b>Names and affiliations of applicants</b> (* indicates experimentalists):  Dr. Peter Rodenbach* (Paul-Drude-Institute, Berlin, Germany) Dipl.-Phys. Martin Dubsloff* (Paul-Drude-Institute, Berlin, Germany) Dr. Paul Fons* (AIST, Tsukuba, Japan) Dr. Michael Hanke* (Paul-Drude-Institute, Berlin, Germany)		

As a report we may provide the following publication, which is exclusively based on the results of the beamtime MA-1236.

P.Rodenbach, A.Giussani, K.Perumal, M.Hanke, M.Dubsloff, H.Riechert, R.Calarco, M.Burghammer, A.V.Kolobov, P.Fons

Recrystallization of an amorphized epitaxial phase-change alloy: A phoenix arising from the ashes  
Appl. Phys. Lett. 101, 061903 (2012)

## Recrystallization of an amorphized epitaxial phase-change alloy: A phoenix arising from the ashes

P. Rodenbach, A. Giussani, K. Perumal, M. Hanke, M. Dubsclaff et al.

Citation: *Appl. Phys. Lett.* **101**, 061903 (2012); doi: 10.1063/1.4742919

View online: <http://dx.doi.org/10.1063/1.4742919>

View Table of Contents: <http://apl.aip.org/resource/1/APPLAB/v101/i6>

Published by the [American Institute of Physics](#).

---

### Related Articles

Substrate-induced disorder in V<sub>2</sub>O<sub>3</sub> thin films grown on annealed c-plane sapphire substrates

*Appl. Phys. Lett.* **101**, 051606 (2012)

High efficiency ultraviolet emission from Al<sub>x</sub>Ga<sub>1-x</sub>N core-shell nanowire heterostructures grown on Si (111) by molecular beam epitaxy

*Appl. Phys. Lett.* **101**, 043115 (2012)

Ultra-low resistance ohmic contacts to GaN with high Si doping concentrations grown by molecular beam epitaxy

*Appl. Phys. Lett.* **101**, 032109 (2012)

Electrical characterization of all-epitaxial Fe/GaN(0001) Schottky tunnel contacts

*Appl. Phys. Lett.* **101**, 032404 (2012)

Epitaxial relationship of semipolar s-plane (101) InN grown on r-plane sapphire

*Appl. Phys. Lett.* **101**, 011904 (2012)

---

### Additional information on *Appl. Phys. Lett.*

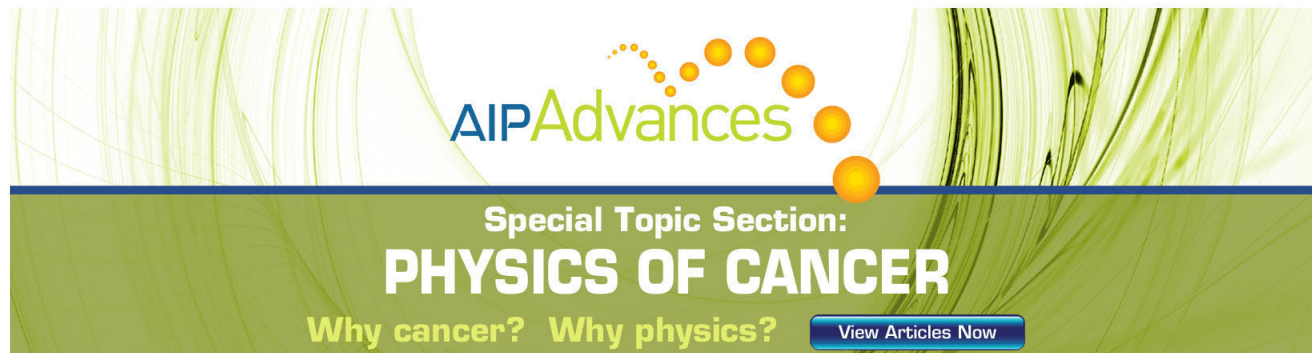
Journal Homepage: <http://apl.aip.org/>

Journal Information: [http://apl.aip.org/about/about\\_the\\_journal](http://apl.aip.org/about/about_the_journal)

Top downloads: [http://apl.aip.org/features/most\\_downloaded](http://apl.aip.org/features/most_downloaded)

Information for Authors: <http://apl.aip.org/authors>

## ADVERTISEMENT

The advertisement features a green and yellow abstract background with flowing lines. At the top, the 'AIP Advances' logo is shown, with 'AIP' in blue and 'Advances' in green, accompanied by a series of orange dots. Below the logo, the text 'Special Topic Section:' is in white, followed by 'PHYSICS OF CANCER' in large, bold, white capital letters. At the bottom, the phrase 'Why cancer? Why physics?' is written in yellow. To the right of this phrase is a blue button with the text 'View Articles Now' in white.

AIP Advances

Special Topic Section:  
**PHYSICS OF CANCER**

Why cancer? Why physics? [View Articles Now](#)

# Recrystallization of an amorphized epitaxial phase-change alloy: A phoenix arising from the ashes

P. Rodenbach,<sup>1,a)</sup> A. Giussani,<sup>1</sup> K. Perumal,<sup>1</sup> M. Hanke,<sup>1</sup> M. Dubslaff,<sup>1</sup> H. Riechert,<sup>1</sup> R. Calarco,<sup>1</sup> M. Burghammer,<sup>2</sup> A. V. Kolobov,<sup>3</sup> and P. Fons<sup>3</sup>

<sup>1</sup>Paul-Drude-Institut für Festkörperelektronik, Hausvogteiplatz 5-7, 10117 Berlin, Germany

<sup>2</sup>European Synchrotron Radiation Facility, 6, rue Jules Horowitz, 38043 Grenoble Cedex 09, France

<sup>3</sup>Nanoelectronics Research Institute, AIST, Tsukuba Central 4, Higashi 1-1-1 Tsukuba, Ibaraki 305-8562, Japan

(Received 14 May 2012; accepted 24 July 2012; published online 6 August 2012)

Epitaxial  $\text{Ge}_2\text{Sb}_2\text{Te}_5$  films grown on Si(111) by molecular beam epitaxy were reversibly switched between crystalline and amorphous states over a large area using femtosecond laser pulses. The structural and spatial homogeneity of the as-grown epitaxial and laser-switched areas on the sample were investigated by synchrotron nanofocus high resolution x-ray diffraction. The investigation clearly demonstrated that the single crystalline metastable cubic phase of  $\text{Ge}_2\text{Sb}_2\text{Te}_5$  is restored after switching. No polycrystalline features, not only on the average but even on the nanometer scale of the x-ray beam, were observed. © 2012 American Institute of Physics. [<http://dx.doi.org/10.1063/1.4742919>]

Advances in multimedia applications and the Internet have driven the development of ever faster and denser memories. One of the most promising approaches is the use of the crystal-to-amorphous phase transition in phase-change materials.<sup>1</sup> In the latter, the property contrast between the crystalline and amorphous phases serves to encode information. Multi-component Te alloys, primarily quasi-binary  $\text{Sb}_2\text{Te}_3$  –  $\text{GeTe}$  alloys, have been identified as the most auspicious class of materials for future electronic memory.<sup>2,3</sup> Those compounds exhibit atypically large differences in optical/electronic properties, excellent scalability, switching speeds, and retention.<sup>4</sup> For  $\text{Ge}_2\text{Sb}_2\text{Te}_5$  (GST) the long-standing consensus on the amorphous phase is that it is obtained by melting the crystalline material by a high-energy laser or current pulse, followed by subsequent rapid cooling, quenching it into an amorphous state whose random structure is representative of the super-cooled liquid.<sup>5</sup> In the re-crystallization process, nuclei driven by thermodynamic fluctuations form with arbitrary orientation leading to the growth of a polycrystalline layer.<sup>6</sup> It is important to note that previous studies of femtosecond (fs) irradiation effects have been performed on samples for which the crystalline phase was obtained by annealing as-deposited amorphous films which are necessarily polycrystalline. The crystallization of sputtered films using fs-laser radiation resulted in a polycrystalline crystal structure as well.<sup>7</sup> Grain boundaries present in these films may affect the properties of the crystalline phase and act to obscure the details of the switching process, i.e., the bond re-arrangements that occur during the formation of the amorphous phase.

To overcome this limitation, in the present study we have investigated the structural properties of as-grown epitaxial and fs-laser-switched single-crystalline samples. The films were subsequently structurally characterized by *nanofocus* high resolution x-ray diffraction (nHRXRD) unambiguously demonstrating that epitaxial  $\text{Ge}_2\text{Sb}_2\text{Te}_5$  can be recrystallized from the amorphous state back into the single-

crystal that it originated from. Molecular beam epitaxy has been employed to fabricate epitaxial phase change films, of composition  $\text{Ge}_2\text{Sb}_2\text{Te}_5$ , in the metastable cubic phase with a unique crystalline orientation. A detailed description of the sample preparation can be found in Ref. 8. The samples investigated in the present work are epitaxial GST films of 50 nm thickness, grown on Si(111), protected with a thin amorphous  $\text{Si}_3\text{N}_4$  cap of 10 nm thickness to prevent oxidation of the layer.

For the switching experiment, the sample was irradiated by light from a regeneratively amplified Ti:Sapphire laser. Laser pulses of 800 nm wavelength were compressed to 180 femtosecond (fs) duration. The pulse power was adjusted by the use of absorption filters. The sample structure was modified by a series of laser pulses. The initial amorphizing pulse had a power density of 12 mJ/cm<sup>2</sup>. The resulting amorphous spot could be recrystallized stepwise by irradiation with lower power density laser pulses of 2 mJ/cm<sup>2</sup>. For the x-ray experiment four different spots on the epitaxial film, each approximately 700  $\mu\text{m}$  in diameter, were prepared.

With the advancement of synchrotron radiation sources, x-ray focusing, employing Si compound refractive lenses, to a beam waist of less than 100 nm has been demonstrated.<sup>9</sup> nHRXRD combines the high resolution structural information from diffraction with nanometer resolved spatial information making scattering information from individual crystal grains accessible. In this study a beam size of less than 150 nm vertically and 200 nm horizontally, at a beam energy of 15.25 keV, was used to spatially resolve the structure within the laser switched areas of epitaxial GST films. The diffraction signal from the sample was recorded in transmission using a fast read out, low noise charge coupled device camera (CCD). Each irradiated spot was scanned using a 71  $\times$  71 position matrix with a 2  $\mu\text{m}$  spacing between positions for a total of 5041 individual images.

Figure 1 presents an investigation of the crystalline state of the as-grown epitaxial film. Fig. 1(a) shows a CCD image of the one second integrated intensity from a single x-ray

<sup>a)</sup>Electronic mail: rodenbach@pdi-berlin.de.

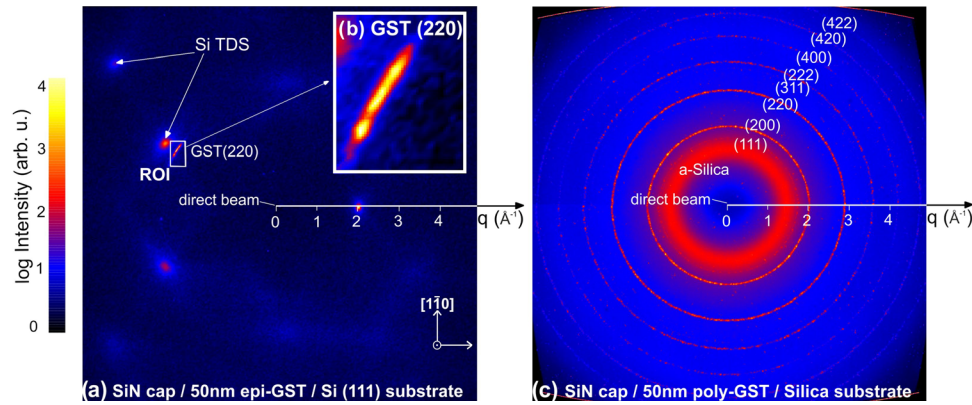


FIG. 1. (a) CCD images recording the diffraction pattern from an epitaxial-GST film at the Bragg angle for the GST (220) netplanes. The only high symmetry direction in the image is the  $[1\bar{1}0]$  direction. The other two directions are only projections of high symmetry directions onto the detector, due to the transmission scattering geometry. (b) The region of interest (ROI) around the epitaxial GST (220) peak magnified for an average diffraction pattern of several position of the x-ray beam on the sample. (c) CCD image of the diffraction from a polycrystalline reference GST film.

spot on the as-grown epitaxial sample. The diffraction from GST (220) netplanes is clearly visible, as highlighted in the magnified image shown in Fig. 1(b). The magnified area is indicated by the white square in the total image of Fig. 1(a). The diffraction peak is sharp and not distributed over a ring; therefore, polycrystalline domains can be excluded on the scale of the beam size. Nevertheless, the peak exhibits an enhanced peak broadening along the angular direction of the scattering vector. In addition to the diffraction from the GST film, a contribution from the thermal diffuse scattering (TDS) in the Si substrate is also visible. All of the bright spots in the image, with the exception of the GST (220) peak, are due to the TDS in the Si substrate and not due to crystal diffraction.<sup>10</sup> The bright spots in reciprocal space are close to reciprocal lattice points of the Si lattice at which the thermal acoustic phonon population is high.<sup>11</sup>

For comparison, Fig 1(c) shows a similar image from a polycrystalline reference GST film deposited by magnetron sputtering. Polycrystalline rings, corresponding to the different GST net planes, are clearly visible. No azimuthal preferred orientation is present; thus, the diffraction intensity is homogeneously distributed over each ring. The granular structure visible within each ring is due to the ultra-fine beam focus which allows the probing of a small number of individual grains, each with an individual orientation. As the center of the camera was aligned to the direct x-ray beam, the magnitude of the scattering vector increases with increasing distance from the center. The scattering vector lengths corresponding to the individual rings match well those reported for the metastable cubic phase of GST.<sup>12</sup>

Figure 2 presents the results of the structural investigation of the laser switched spots in the epitaxial GST film by nHRXRD. The spatial shape of the laser spot is ideally a Gaussian function in the two lateral dimensions on the sample surface; however, due to the presence of several optical elements in the laser setup the beam shape is somewhat distorted. As the epitaxial layer is grown in the metastable cubic form, the first high power laser pulse serves to amorphize the crystalline layer. Fig. 2(a) shows an optical micrograph of a spot that was amorphized with one high power pulse, surrounded by a large area of the epitaxial cubic film. Due to the large optical contrast between the amorphous and crystal-

line material the amorphous mark is apparent. Fig. 2(b) is a higher resolution micrograph of again a spot that was amorphized with one high power pulse. Fig. 2(d) is an optical image of a spot that was amorphized with one high power pulse and subsequently irradiated by ten low power recrystallization pulses, respectively (for recrystallization, a single pulse did not fully recrystallize the spot, hence the necessity to use 10 pulses; larger numbers of pulses had no further effect on the crystallinity). On the right of the optical microscopy images, the corresponding spatially resolved diffraction information (Figs. 2(c) and 2(e)) for each investigated laser spot is shown. For the construction of the spatial x-ray image, the normalized integrated intensity of the GST (220) peak for the region of interest indicated in Fig. 1(b) was evaluated, and this value was plotted at the position in the image corresponding to the spatial position of the x-ray beam on the sample. In short, for each spatial position of the x-ray beam on the sample the intensity in the GST (220) Bragg peak is plotted. Each laser spot was sampled using the nanobeam at a  $71 \times 71$  matrix of positions spaced by  $20 \mu\text{m}$ .

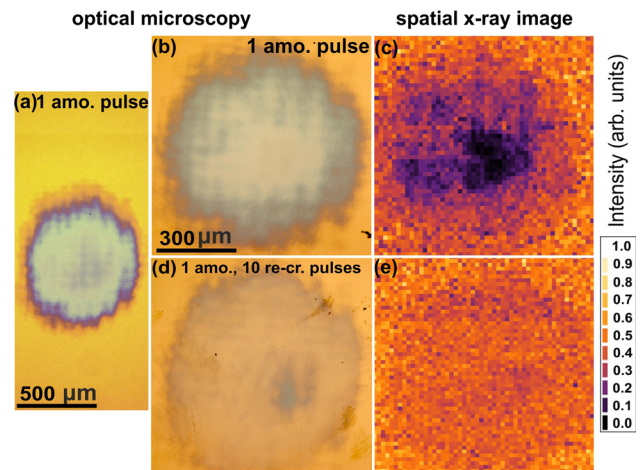


FIG. 2. Overview micrograph of a single pulse amorphized spot surrounded crystalline material (a). Comparison of optical micrographs of the laser switched spots (b),(d), and the corresponding spatially resolved x-ray diffraction images (c),(e); the two spots were exposed to different pulse sequences. The spatially resolved x-ray image shows the integrated intensity of the GST (220) peak for each spatial position of the x-ray beam on the laser spot.



In optical microscopy the amorphous regions in the spot appear optically darker due to the higher reflectivity of the crystalline state of GST in the visible light range. In x-ray diffraction, the amorphous regions appear less intense as well, due to the reduced number of coherent x-ray scatterers. Only at the very central region of the laser-spot does the x-ray intensity of the GST (220) peak completely vanish into the background. This indicates that the laser penetration depth in the layer is not uniform over the entire spot and extends through the entire layer thickness only in the center region.

After the initial high intensity amorphization pulse (amo. pulse), the central part of the spot appears much darker (Fig. 2(b)). The gray area in the optical images at the edges of the laser spot are attributed to structurally mixed areas with both amorphous and crystalline regions at different depths in the film. Exposing the amorphous spot to 10 recrystallization pulses reverts it to a higher reflectivity state as shown in Fig. 2(d). The reflectivity is similar to, but different from the reflectivity of the as-grown crystalline state.

Evaluating the structural information yields the same result (Fig. 2(e)). The absolute intensity of the GST (220) Bragg peak returns on average 95% of its initial value in the as-grown epitaxial form. As the integration region around the GST (220) Bragg peak defines a very limited region in reciprocal space and excludes any polycrystalline contribution, the crystal lattice in the laser-spot unambiguously returns to its single-crystalline form. This behavior has been confirmed for other Bragg peaks such as the (11 $\bar{1}$ )-peak (not shown). As the beam probes the structure on the nanometer scale, this statement is true for all individual grains probed by the x-ray beam and consequentially the average as well. The remaining grayish areas at the edges of the laser spot at the border of the non-switched as-grown epitaxial films contain small remaining amorphous regions which are attributed to inhomogeneities in the intensity of the laser. It is noted that optical reflectivity is very sensitive to phase shifts at interfaces and hence offers little sensitivity to amorphous regions deeper in the sample.

A detailed investigation of the Bragg peaks reveals a lattice constant of 5.93(5) Å for as-grown epitaxial GST with a NaCl-type unit cell, which is 1.3(6)% smaller than the literature value for polycrystalline GST of 6.012 Å.<sup>13</sup> In the recrystallized regions the diffraction intensity returns to a value close to that of the as-grown epitaxial sample, but with a small shift of the peak position. The lattice relaxes towards a larger lattice constant by about 1.2% resulting in a final lattice d-spacing of 6.01(5) Å in agreement with the polycrystalline value. For GST films that were crystallized from sputtered amorphous material on an amorphous glass substrate using fs-laser pulses, the resulting structure was found to be polycrystalline with slightly smaller lattice d-spacings than the crystalline structure of the same films obtained by annealing.<sup>7</sup> This reflects the strong influence of the Si(111) template during epitaxy for single crystal GST. The half-width of the peaks also slightly increase, corresponding to a reduction in the domain size after recrystallization. There are different possible explanations as to why the integrated x-ray intensity does not return to 100% of its initial value. First, the entire volume of the spot may not have switched back along the film depth direction, as the layer thickness exceeds the pene-

tration depth of the laser beam, in addition to the non-ideal beam profile of the switching laser. Second, the observed shift of the lattice constant of 1.3% corresponds to an altered electron density and reflectivity, respectively. Beam damage to the film due to the high x-ray intensity becomes significant after 50 s of continuous exposure at a fixed position and is thus negligible for the present results for which the maximum exposure time per position amounted to 2 s.

In conclusion, nHRXRD non-destructively revealed the crystal structure of epitaxial Ge<sub>2</sub>Sb<sub>2</sub>Te<sub>5</sub> on Si(111) on the nanometer scale of the beam size. Most notably, the observation that the intensity fully recovers in the small region of interest defined around the asymmetric (220) Bragg peak unambiguously demonstrates that the single crystalline domains completely recover their initial out-of-plane and in-plane orientation, despite the fact that homogeneous nucleation has been reported to be the dominant crystallization process in Ge<sub>2</sub>Sb<sub>2</sub>Te<sub>5</sub> which ought to result in a polycrystalline layer.<sup>6</sup> This result demonstrates that the amorphous phases possess latent memory of the initial crystalline phase, or the influence of the single crystal interface plays a crucial role in the crystal nucleation and subsequent growth. Upon recrystallization, the positions of the peaks in reciprocal space demonstrate that the lattice constant changes towards the literature powder value within the accuracy of the experiment upon recrystallization. The diffraction peak slightly broadens and the maximum peak intensity decreases, while the integrated intensity fully recovers. This indicates a decrease of the in-plane domain size during recrystallization, as qualitatively supported by a domain size analysis. Further studies are currently underway.

The authors acknowledge the technical support of S. Behnke, C. Stemmler. Support for this work was provided by the Deutsche Forschungsgemeinschaft (CA 664/3-1), the Deutsche Akademische Austauschdienst, and the European Synchrotron Radiation Facility (MA-1236).

<sup>1</sup>M. Wuttig and N. Yamada, *Nat. Mater.* **6**, 824 (2007).

<sup>2</sup>T. Ohta and S. R. Ovshinsky, "Photo-induced metastability in amorphous semiconductors," *Phase-Change Optical Data Storage Media* (Wiley-VCH, 2003), pp. 310–326.

<sup>3</sup>D. Lencer, M. Salinga, B. Grabowski, T. Hickel, and M. Wuttig, *Nat. Mater.* **7**, 972 (2008).

<sup>4</sup>A. Lacaita, *Sol. State Electron.* **50**, 24 (2006).

<sup>5</sup>S. Raoux, W. Welnic, and D. Ielmini, *Chem. Rev.* **110**, 240 (2010).

<sup>6</sup>J. Coombs, A. Jongenelis, W. van Es-Spiekman, and B. Jacobs, *J. Appl. Phys.* **78**, 4906 (1995).

<sup>7</sup>G. Zhang, D. Gu, F. Gan, X. Jiang, and Q. Chen, *Thin Solid Films* **474**, 169 (2005).

<sup>8</sup>P. Rodenbach, R. Calarco, K. Perumal, F. Katmis, M. Hanke, A. Proessdorf, W. Braun, A. Giussani, A. Trampert, H. Riechert, P. Fons, and A. Kolobov, "Epitaxial phase change materials: new perspectives," *Cryst. Growth Des.* (submitted).

<sup>9</sup>M. Dubschlaff, M. Hanke, M. Burghammer, S. Schöder, R. Hoppe, C. G. Schroer, Y. I. Mazur, Z. M. Wang, J. H. Lee, and G. J. Salamo, *Appl. Phys. Lett.* **98**, 213105 (2011).

<sup>10</sup>J. Als-Nielsen and D. McMorrow, *Elements of Modern X-Ray Physics*, 2nd ed. (John Wiley & Sons Ltd., 2011).

<sup>11</sup>M. Holt, Z. Wu, H. Hong, P. Zschack, P. Jemian, J. Tischler, H. Chen, and T.-C. Chiang, *Phys. Rev. Lett.* **83**, 3317 (1999).

<sup>12</sup>N. Yamada, E. Ohno, K. Nishiuchi, N. Akahira, and M. Takao, *J. Appl. Phys.* **69**, 2849 (1991).

<sup>13</sup>T. Nonaka, G. Ohbayashi, Y. Toriumi, Y. Mori, and H. Hashimoto, *Thin Solid Films* **370**, 258 (2000).